Biogeosciences Discuss., 12, 19535–19577, 2015
www.biogeosciences-discuss.net/12/19535/2015/
doi:10.5194/bgd-12-19535-2015

Biogeosciences Discussions
Open Access
EGU

Modeling the uncertainty of estimating forest carbon stocks in China

T. X. Yue[1,2], Y. F. Wang[1,2], Z. P. Du[1], M. W. Zhao[3], L. L. Zhang[1,2], N. Zhao[1], M. Lu[1,2], G. R. Larocque[4], and J. P. Wilson[1,5]

[1]State Key Laboratory of Resources and Environment Information System, Institute of Geographical Science and Natural Resources Research, Chinese Academy of Sciences, 11A, Datun Road, Beijing, 100101, China
[2]University of Chinese Academy of Sciences, 19A, Yuquan Road, Beijing 100049, China
[3]Anhui Center for Collaborative Innovation in Geographical Information Integration and Application, Chuzhou University, 1528, Fengle Road, Chuzhou, Anhui, 239012, China
[4]Natural Resources Canada, Canadian Forest Service, Laurentian Forestry Centre, 1055 du P.E.P.S., G1V 4C7, Canada
[5]Spatial Sciences Institute, Dana and David Dornsife College of Letters, Arts and Sciences, University of Southern California, Los Angeles, USA

Received: 16 October 2015 – Accepted: 7 November 2015 – Published: 10 December 2015

Correspondence to: T. X. Yue (yue@lreis.ac.cn)

Published by Copernicus Publications on behalf of the European Geosciences Union.

Abstract

Earth surface systems are controlled by a combination of global and local factors, which cannot be understood without accounting for both the local and global components. The system dynamics cannot be recovered from the global or local controls alone. Ground forest inventory is able to accurately estimate forest carbon stocks at sample plots, but these sample plots are too sparse to support the spatial simulation of carbon stocks with required accuracy. Satellite observation is an important source of global information for the simulation of carbon stocks. Satellite remote-sensing can supply spatially continuous information about the surface of forest carbon stocks, which is impossible from ground-based investigations, but their description has considerable uncertainty. In this paper, we validated the Lund-Potsdam-Jena dynamic global vegetation model (LPJ), the Kriging method for spatial interpolation of ground sample plots and a satellite-observation-based approach as well as an approach for fusing the ground sample plots with satellite observations and an assimilation method for incorporating the ground sample plots into LPJ. The validation results indicated that both the data fusion and data assimilation approaches reduced the uncertainty of estimating carbon stocks. The data fusion had the lowest uncertainty by using an existing method for high accuracy surface modeling to fuse the ground sample plots with the satellite observations (HASM-SOA). The estimates produced with HASM-SOA were 26.1 and 28.4 % more accurate than the satellite-based approach and spatial interpolation of the sample plots, respectively. Forest carbon stocks of 7.08 Pg were estimated for China during the period from 2004 to 2008, an increase of 2.24 Pg from 1984 to 2008, using the preferred HASM-SOA method.

1 Introduction

Biomass dynamics reflect the potential of vegetation to act as a carbon sink over the long-term, as they integrate photosynthesis, autotrophic respiration and litter fall fluxes

(Thurner et al., 2014). Forest ecosystems cover more than 41 million km^2 of the Earth's land surface and forests are thought to contain about half of the carbon in terrestrial biomes (Prentice et al., 2001). Forests play an important role in the active mitigation of atmospheric CO_2 through increased carbon stocks. The fixation of atmospheric CO_2 into plant tissue through the process of photosynthesis is one of the most effective mechanisms for offsetting carbon emissions (Canadell and Raupach, 2008; Gonzalez-Benecke et al., 2010).

Carbon sequestration by trees is the best way to store a large amount of terrestrial carbon over long durations (Jung et al., 2013). Understanding carbon stocks and the underlying driving forces at scales ranging from local to global is crucial for accurately predicting future changes in atmospheric carbon dioxide (Yu et al., 2014). However, substantial uncertainties remain in current model estimates of terrestrial carbon and there is an increasing need to quantify and reduce these uncertainties (Barman et al., 2014; Ahlstrom et al., 2012).

This represents a substantial challenge given the large number and variety of methods and data that have been used to prepare estimates of terrestrial carbon thus far. Five kinds of approaches – ground-observation-based estimation, satellite-based estimation, mechanism models, mechanism models combined with ground and/or satellite observations, and the fusion of ground and satellite observations – can be distinguished and the commentary that follows show how each of these approaches has been used to estimate carbon stocks in various areas with varying levels of uncertainty to date.

Many of the ground-observation based studies have used allometric regression models to convert forest inventory data to estimates of aboveground biomass with varying levels of success (e.g., Chave et al., 2005; Strand et al., 2008; van Breugel et al., 2011). Validation in Colombian forests, for example, indicated that the standard deviation of the total biomass estimates was 39.1 % when the allometric model included only tree diameter at breast height (D) as an explanatory variable, < 25.6 % when the total height (H) of the trees, wood density (ρ) and D were used as explanatory

BGD
12, 19535–19577, 2015

variables, and 35.7 % when ρ and D were used as explanatory variables (Alvarez et al., 2012). Sierra et al. (2007) estimated the uncertainty of estimates of total carbon stocks for the tropical forest of Colombia at 11 % for primary forests and 5 % for secondary forests using Monte Carlo simulation. In another study, Kearsley et al. (2013) determined that aboveground carbon stocks would be over-estimated by 24 % in the Central Congo Basin if the best available H–D relationships derived for Central Africa were used. And finally, Navar (2009) found that the total variation of biomass explained by allometric equations was 89 % on average for forests in northwestern Mexico.

The problem or challenge with this kind of approach is that the estimates of carbon stocks are usually based on the upscaling of sparse forest inventory data (Liski et al., 2000; Thurner, 2014). Such approaches provide poor spatial resolution and high uncertainty because forest inventories are always limited, especially in remote areas. For example, the aboveground woody carbon accumulation rate was estimated to be $10.0\,\mathrm{g\,C\,m^{-2}\,yr^{-1}}$ on the Owyhee Plateau of southwestern Idaho in the US during the period 1946–1998 based on a wavelet and texture method, but only $3.3\,\mathrm{g\,C\,m^{-2}\,yr^{-1}}$ based on field collection data (Strand et al., 2008). Similarly, the uncertainty of plot-based estimates of carbon change in a temperate rainforest in New Zealand was 78.1 % (Holdaway et al., 2014) and a standardized inventory of total carbon storage in boreal forests (Bradshaw and Warkentin, 2015) was between 1.3 and 3.8 times larger than any previous mean estimates (Apps et al., 1993; Pan et al., 2011). Some recent work has improved the accuracy of ground-observation-based carbon stock estimates. For instance, the Global Wood Density database has improved the accuracy of regional wood density estimates used for carbon stock assessments by 17 % (Flores and Coomes, 2011) and the component ratio method decreased the uncertainties of US forest carbon stock estimates by an average of 16 % (Domke et al., 2012).

Satellite-observation based methods have been widely used for the estimation of aboveground forest carbon stocks, due to the better availability, broad coverage and finer temporal resolution they offer compared to conventional field surveying (Heo et al., 2006; Hyyppä et al., 2000; Tomppo and Halme, 2004).

BGD
12, 19535–19577, 2015

Air- and space-borne remote sensing platforms provide continuous spatial information over large areas in contrast to field inventory where information is generally limited to plots or small areas (Petrokofsky et al., 2012). Remote sensing methods have been used for land cover discrimination to monitor reforestation and/or deforestation and to estimate aboveground forest carbon stocks. For land cover discrimination, both optical and radar remote sensing have proved successful. For forest carbon stock estimation, radar is most appropriate, at least until light detection and ranging (LiDAR) is made available from satellite platforms (Patenaude et al., 2005). In one such application, a forest carbon density map at a spatial resolution of 0.01° was created using radar remote sensing and used to estimate carbon stocks in Northern Hemisphere boreal and temperate forests. The uncertainty of these estimates fell within the range of 30–40 % (Thurner et al., 2014).

Similarly, WorldView-2 satellite imagery was integrated with small footprint airborne LiDAR data to estimate tree carbon at the species level in the tropical forest of Nepal. The validation results showed that the regression models which incorporated the first and last LiDAR returns were able to explain up to 94, 78, 76, 84 and 78 % of the variations in carbon estimates for the four dominant tree species – *Shorea robusta, Lagerstroemia parviflora, Terminalia tomentosa, Schima wallichii* – and other tree species, respectively (Karna et al., 2015). These kinds of results are promising; however, a comprehensive crowd-sourced survey in Guyana indicated that estimates based on remotely sensed data may be less accurate than is commonly assumed (Butt et al., 2015).

A large number and variety of mechansim-based simulation models have also been proposed and used to estimate forest carbon stocks. The Physiological Principles in Predicting Growth (3-PG) model, for example, calculates the total carbon fixed from utilizable, absorbed photosynthetically active radiation, obtained by correcting the photosynthetically active radiation absorbed by the forest canopy for the effects of soil drought, atmospheric vapor pressure deficits, and stand age (Landsberg and Waring, 1997). Validation using age-related changes in carbon storage and allocation

BGD
12, 19535–19577, 2015

in a Chinese fir plantation growing in southern China indicated that this particular model predicted approximately 90 % of the variability in field measurements for tree diameter at breast height and litterfall (Zhao et al., 2009). The Biome-BGC (biogeochemical cycles) model, on the other hand, extends the Forest-BGC model (Running and Coughlan, 1988) and simulates above- and below-ground carbon, water, and nitrogen cycles for different vegetation types. This model is strongly controlled by LAI and climate (Schmid et al., 2006) and has been validated in grassland sites in Hungary and two independent forest sites in Italy, yielding correlation coefficients between measurement and simulation data of 0.81 in grassland ecosystems (Hidy et al., 2012) and 0.83 at forested sites (Chiesi et al., 2007).

Several Dynamic Global Vegetation Models (DGVMs) have also been developed by various research groups. These include LPJ (Sitch et al., 2003), IBIS (Foley et al., 1996; Kucharik et al., 2000), MC1 (Daly et al., 2000), HYBRID (Friend et al., 1995), SDGVM (Woodward et al., 1998), VECODE (Brovkin et al., 1997), and ED (Moorcroft et al., 2001; Medvigy et al., 2009). These models use time series of climate data and given constraints of latitude, topography and soil characteristics, simulate the monthly or daily dynamics of ecosystem processes with varying levels of uncertainty. An Integrated Science Assessment Model (ISAM) has also been developed by combining biogeochemical components with the detailed biogeophysical schemes of land surface models (Barman et al., 2014). Validation studies have shown that annual Gross Primary Production (GPP) bias at tropical evergreen tree sites was 15 % of site level GPP, increasing to 20 % at northern mid- and high-latitude broadleaf deciduous and needleleaf evergreen tree sites, and 20–30 % for non-tree sites with savanna, grass, and shrub land vegetation types. The Carbon Budget Model of the Canadian Forest Sector (CBM-CFS3), on the other hand, incorporates a forest C budgeting framework that can be applied at the stand-, regional-, and national-scales (Kurz et al., 2009). The ecosystem total C stocks estimated by CBM-CFS3 explained just 54 % of the variability in ground plot-based estimates (Shaw et al., 2014).

And finally, an innovative and forward-looking Game-Theoretic Allocation Model (GTAM) has been used to investigate how: (1) optimally competitive tree allocation would change in response to elevated atmospheric CO_2 along a gradient of nitrogen and light availability; and (2) how those changes would affect carbon storage in living biomass (Dybzinski et al., 2015). The application of GTAM using local information incorporates considerable uncertainty because trees competitively allocate carbon and nutrients differently under differing constraints of water, nutrients, light, and CO_2 availability (Dybzinski et al., 2011, 2013; Franklin et al., 2012; Farrior et al., 2013; McMurtrie and Dewar, 2013). However, the acquisition of global information on multiple resource constraints may help to reduce the uncertainty of mechanism-based predictions of carbon sequestration in the future.

Several studies have also proposed methods that combine ground-observation, satellite-observation, and mechanism-based models to estimate carbon stocks. Satellite-based remote sensing data can be combined with field observations on a pixel-by-pixel basis, for example, to provide more accurate estimates of the spatial distributions of forest biomass and carbon stocks (Jung et al., 2013). Hence, Liu et al. (2002) estimated the annual carbon sources and sinks in Canada's forests at a 1 km^2 resolution for the period 1901–1998 using the Boreal Ecosystem Productivity Simulator (BEPS) that integrates remote sensing imagery, gridded climate, soils and forest inventory data. The results showed the simulated aboveground biomass values for mixed and deciduous forest types were about 30 % larger than the inventory data for Canada's forests (Liu et al., 2002; Chen et al., 2003). Stuemer et al. (2010) also combined satellite remote sensing data with in situ national forest inventory data to estimate aboveground woody biomass and forest carbon stocks for a test site in Thuringia, Germany. The k nearest neighbor (kNN) method was used to expand the terrestrial point observations and provide spatially explicit wall-to-wall coverage by utilizing similarities in the spectral image space of the remote sensing data. Validation results showed that the relative root mean square errors (RMSEs) of the self-organizing

BGD
12, 19535–19577, 2015
Modeling the uncertainty of estimating forest carbon stocks in China
T. X. Yue et al.

map (SOM) and the kNN method ranged between 66.3 and 70.49, and 44.85 and 55.58 %, respectively (Stuemer et al., 2010).

Several other approaches have fused ground- and satellite-observation data within one or more formal models. Yuan et al. (2007), for example, used the light use efficiency (LUE) daily GPP model from eddy covariance (EC) measurements. This EC-LUE model is driven by four variables: (1) NDVI; (2) photosynthetically active radiation (PAR); (3) air temperature; and (4) the Bowen ratio of sensible to latent heat flux. The model was calibrated and validated using 24 349 daily GPP estimates derived from 28 eddy covariance flux towers in the AmeriFlux and EuroFlux networks, and the results showed that EC-LUE explained 85 and 77 % of the observed variations in daily GPP for the calibration and validation sites, respectively. The GloPEM model has also been used to estimate GPP (Prince and Goward, 1995; Singh et al., 2011). This model is based on physiological principles and uses satellite-based remotely sensed data with the production efficiency concept, in which the canopy absorption of photosynthetically active radiation (APAR) is used with a conversion "efficiency", to estimate GPP. The Carnegie Ames Stanford Approach (CASA), on the other hand, simulates light-use efficiency and has been applied using AVHRR satellite data at a regional scale to estimate seasonal and annual carbon fluxes as Net Primary Production (NPP) (Potter et al., 1993, 2011). Applications of the GloPEM and CASA models in China, however, produced relative errors of annual mean NPP of ~ 35 % (Gao and Liu, 2008).

This particular article describes a series of experiments to model the uncertainty associated with estimating forest carbon stocks in China. There were three goals as follows:

1. To choose a variety of methods for estimating carbon stocks and to calculate the uncertainty associated with each of these methods.

2. To choose and compare the best estimates at the national scale with previously published estimates.

3. To examine the variability in forest carbon stocks by region and forest type.

BGD
12, 19535–19577, 2015

The choice of forest carbon stocks in China was important given the large size and fast pace of change in China and the importance of terrestrial vegetation and particularly forests as a way to mitigate rising CO_2 levels in the atmosphere. The remainder of this article is divided into four parts: Sect. 2 reviews previously published estimates of carbon stocks in China; Sect. 3 describes the overall experimental design and the specific methods and data that were used in this work; Sect. 4 reports the results, and the fifth and final section summarizes the major findings and offers some suggestions for future work.

2 Previously published estimates of forest carbon stocks in China

Several studies have estimated the forest carbon stocks in China using one of the aforementioned estimation methods.

Piao et al. (2005), for example, used a satellite-based approach and estimated that: (1) the total forest biomass of China averaged 5.79 Pg C during the period 1981–1999, with an average biomass density of 4.531 $kg\,C\,m^{-2}$; and (2) the total forest biomass C stock increased from 5.62 Pg C in the early 1980s to 5.99 Pg C by the end of the 1990s, giving a total increase of 0.37 Pg C and an annual sequestration rate of 19 $Tg\,C\,yr^{-1}$. Zhang et al. (2007), on the other hand, analyzed seven forest inventories from 1973 to 2008 and suggested that the total biomass carbon stocks of all forest types increased by 65 % during this period, reaching 8.12 Pg C in 2008.

Wang et al. (2007) used the Integrated Terrestrial Ecosystem C-budget model and estimated that China's forests were a source of $21.0 \pm 7.8\,Tg\,C\,yr^{-1}$ due to human activities during the period 1901–1949 and that this flux increased to $122.3 \pm 25.3\,Tg\,C\,yr^{-1}$ due to intensified human activities during the period 1950–1987. However, these forests became large sinks of $176.7 \pm 44.8\,Tg\,C\,yr^{-1}$ during the period 1988–2001 owing to large-scale plantation and forest regrowth in previously disturbed areas (see the description of the Grain for Green Program below) as well as climatic warming, atmospheric CO_2 fertilization, and N deposition.

BGD
12, 19535–19577, 2015

Yang and Guan (2008), on the other hand, utilized the continuous Biomass Expansion Factor (BEF) method with field measurements of forests plots in different age classes and forest inventory data, and showed that the carbon density of the forests in the Pearl River Delta increased by 14.3 % from 19.08 to 21.81 $kg\,C\,m^{-2}$ during the period 1989–2003. Similarly, Piao et al. (2009) reported that China's terrestrial ecosystems were a net carbon sink of 0.19–0.26 $Pg\,C\,yr^{-1}$ and that they absorbed 28–37 % of the fossil carbon emissions during the 1980s and 1990s. However, their results also showed that northeast China is a net source of CO_2 to the atmosphere due to the over-harvesting and degradation of forests, while southern China accounts for more than 65 % of the carbon sink, which can be attributed to regional climate change, large-scale plantation programs started in the 1980s, and shrub recovery (Piao et al., 2009).

Guo et al. (2010) used three different approaches – the mean biomass density (MBD), the mean ratio (MR), and the continuous biomass expansion factor (BEF) method (CBM) – with forest inventory data to estimate China's forest biomass C stocks and their changes from 1984 to 2003. The MBD, MR, and BEF estimated that forest biomass C stocks increased from 5.7 to 7.7, 4.2 to 6.2, and 4.0 to 5.9 Pg C, respectively.

Deng et al. (2011) deployed a GIS approach and defined the vegetation carbon sink as the carbon sequestration from the atmosphere (1.63 × NPP), the vegetation carbon stock as the carbon content that aboveground vegetation holds, and the soil carbon stock as the carbon content that soil organic matter holds. These author's estimated vegetation and soil carbon stocks of 1.58 and 1.41 Pg C, respectively in the forest ecosystems of China for the period 1981–2000.

Ni (2013) used available national-scale information to estimate that: (1) the mean vegetation carbon in China was 36.98 Pg and mean soil carbon was 100.75 Pg C; and (2) that the forest and grassland sectors supported mean carbon stocks of of 5.49 and 1.41 Pg C, respectively.

The aforementioned studies show that the forest ecosystems of China store steadily increasing stocks of carbon and that these forest stands have great potential to absorb

BGD
12, 19535–19577, 2015

more biomass carbon in the future due to large fractions of young and middle-aged forests and programs to promote the conservation of soil and biological resources.

The Grain for Green program, which was launched in 1999 and aims to restore the country's forests and grasslands to prevent soil erosion, has emerged as one of the key drivers of carbon sequestration. This program targets land with slopes > 25° (Xu et al., 2006; Yue et al., 2010c) and has been implemented in four phases: (1) a pilot phase (1999–2001); (2) an initial construction phase (2002–2010); (3) a consolidation phase (2011–2013); and (4) a second construction phase to be built around a new round of Grain for Green program expenditures (2014–2020).

The pilot program launched in 1999 focused on three provinces: Gansu, Shaanxi and Sichuan. Approximately 381 000 ha of farmland was converted into forestland and 66 000 ha of bare land was reforested. In 2000, the program was expanded to 17 provinces, and the converted farmland and reforested bare land totals grew to 410 000 and 449 000 ha, respectively. By 2001, 20 provinces were involved in the program and 420 000 and 563 000 ha of farm and bare land had been reforested, respectively (Table 1). The national Grain for Green program was launched in China in 2002 and by the end of 2010, 14.667 million ha of farmland had been converted to forest or grassland and 17.333 million ha of bare land had been reforested. During the consolidation phase from 2011 to 2013, scientific monitoring and management of the converted and reforested lands was strengthened to sustain the aforementioned achievements of the Grain for Green program over the long-term.

To grow and consolidate these gains, the potential for farmland conversion at the county level during the period 2014–2020 was estimated in 2014 by counting up farmers' voluntary applications to determine how large an area could be converted to forest or grassland. By 2020, 2.827 million ha of farmland could be converted, which includes 1.449 million ha of farmland with slopes > 25°, 1.133 million ha of cultivated land threatened by desertification, and 247 000 ha of farmland with slopes between 15 and 25° around the Danjiangkou and Three Gorges reservoirs.

BGD
12, 19535–19577, 2015

The results from this latest phase of the Grain for Green program are encouraging. Participating farmers can choose whether farmland is to be converted to forest or grassland, and which species will be planted, and they will receive a CNY 22 500 subsidy for every hectare of farmland converted to forest or grassland. In 2014, 322 000 ha were converted to forest and 11 000 ha were converted to grassland, and in 2015 another 667 000 ha of farmland will be converted to either forest or grassland.

All these published results relied on either ground- or satellite-observation-based estimation unlike our own work in which we have tried to fuse these data sources to reduce the uncertainty associated with the final carbon stock estimates.

3 Experimental design

3.1 Forest distribution data

The forest distribution database of China was created using the Vegetation Atlas of China (Editorial Board of Vegetation Map of China, 2001) and the European Space Agency's GlobCover 2009 database (http://globalchange.nsdc.cn). The forest distribution data covers 161 plant biomes, including five classes of deciduous needle-leaved trees, 57 classes of evergreen needle-leaved trees, 39 classes of deciduous broad-leaved trees, 56 classes of evergreen broad-leaved trees and four classes of mixed trees (Fig. 1).

3.2 Forestry inventory database (FID)

The national FID for the period 2004–2008 includes 160 000 permanent sample plots and 90 000 temporary sample plots scattered across China. The biomass density of each forest type in each province was calculated from timber volume, using a BEF (Table 2). The carbon density (CD) of each forest type in each province was calculated next by multiplying the biomass density by a carbon factor (CF) (Table 3). And finally, the carbon stocks (CS) of each forest type in each province were calculated by

BGD
12, 19535–19577, 2015

multiplying the CD by the area of that forest type. The total CS in China is a sum of the CS of all of the forest types in the 31 provinces of China, excluding Taiwan, Hong Kong and Macao.

The following formulations were used to calculate the forest CS in China:

$$\mathrm{TCS} = \sum_{i=1}^{M}\sum_{j=1}^{N}(A_{i,j} \times \mathrm{BCD}_{i,j}) \times 10^{-12} \tag{1}$$

$$\mathrm{BCD}_{i,j} = W_{i,j} \times \mathrm{CF}_i \tag{2}$$

$$W_{i,j} = \mathrm{BEF}_i \times V_{i,j} \tag{3}$$

$$\mathrm{BEF}_{i,j} = a_i + \frac{b_i}{V_{i,j}} \tag{4}$$

where TCS is the total forest CSs of China (Pg); $\mathrm{BCD}_{i,j}$ is the area weighted mean biomass CD of the ith forest type in the jth province ($\mathrm{kg\,m^{-2}}$); $A_{i,j}$ is the area of the ith forest type in the jth province ($\mathrm{m^2}$); M and N refer to the numbers of forest types and provinces in China, respectively; $W_{i,j}$ is the area weighted mean forest biomass of the ith forest type in the jth province ($\mathrm{kg\,m^{-2}}$); CF_i is the CF of the ith forest type; $V_{i,j}$ is the area weighted mean timber volume of the ith forest type in the jth province ($\mathrm{m^3\,m^{-2}}$); BEF_i is the BEF of the ith forest type ($\mathrm{kg\,m^{-3}}$); and a_i ($\mathrm{kg\,m^{-3}}$) and b_i ($\mathrm{kg\,m^{-2}}$) are constants of the ith forest type to be simulated.

The mean CF_i of all coniferous forest types was used for coniferous mixed forest. The mean CF_i of all broad-leaved forest types was used for broad-leaved mixed forest. The mean CF_i of all broad-leaved and coniferous forest types was used for broad-leaved and coniferous mixed forest.

3.3 Satellite-observation-based approach (SOA)

The SOA used the monthly NDVI at a spatial resolution of 1 km × 1 km from the Earth Observation System's moderate-resolution imaging spectroradiometer (EOS MODIS)

BGD
12, 19535–19577, 2015

Discussion Paper | Discussion Paper | Discussion Paper | Discussion Paper |
Title Page
Abstract Introduction
Conclusions References
Tables Figures
◀ ▶
Back Close
Full Screen / Esc
Printer-friendly Version
Interactive Discussion

(Piao et al., 2009). The CD from the FID data was matched with the NDVI data through the updated map of forest in China reproduced in Fig. 1.

The biomass carbon density (BCD) mirrored the latitude, longitude and maximum value of the monthly-averaged NDVI values during the Seventh National Forest Inventory conducted from 2004 to 2008:

$$\mathrm{BCD}_j = 93.351\ln(\mathrm{NDVI}_j) - 2.96\mathrm{Lat}_j - 21.388\mathrm{Lon}_j + 0.047\mathrm{Lat}_j^2 + 0.091\mathrm{Lon}_j^2 + 1339.03 \tag{5}$$

where NDVI_j is the mean of the maximum values of the monthly-averaged NDVI values during the period 2004–2008 in the jth province and Lat_j and Lon_j refer to the latitude and longitude of the center of the jth province, respectively. The coefficient of correlation ($R = 0.91$) and significance ($P < 0.001$) show how latitude, longitude, and NDVI explained 83 % of the variability in BCD.

3.4 Lund-Potsdam-Jena dynamic global vegetation model (LPJ-DGVM)

The LPJ-DGVM (Sitch et al., 2003) was also implemented and used to estimate the carbon stocks of China. This particular model combines process-based, large-scale representations of terrestrial vegetation dynamics and land–atmosphere carbon and water exchanges in a modular framework as a component of coupled Earth system models. It has been used to simulate global totals and spatial distributions of soil, litter and vegetation carbon pools and net primary production at a spatial resolution of $0.5^\circ \times 0.5^\circ$ (Cramer et al., 2001; Sitch et al., 2003; Venevsky and Maksyutov, 2007). An investigation into spatio-temporal carbon balance patterns resulting from forcing LPJ with output from 18 climate models of the CMIP5 (Coupled Model Intercomparison Project Phase 5) ensemble showed that the terrestrial biosphere becomes a net source of carbon in 10 of the 18 simulations adding to the atmospheric CO_2 concentrations, while the remaining eight simulations indicate the terrestrial biosphere becomes a net sink for carbon (Ahlstroem et al., 2012).

BGD
12, 19535–19577, 2015

3.5 High accuracy surface modeling (HASM)

HASM was developed for efficiently fusing satellite- with ground-observations to find solutions for error problems which have long troubled earth surface modeling (Yue, 2011). HASM has been successfully used to construct digital elevation models (Yue et al., 2007, 2010a, b; Yue and Wang, 2010; Chen and Yue, 2010; Chen et al., 2013a, b), model surface soil properties (Shi et al., 2011) and soil pollution (Shi et al., 2009), fill voids in the Shuttle Radar Topography Mission (SRTM) dataset (Yue et al., 2012), simulate climate change (Yue et al., 2013a, b; Zhao and Yue, 2014a, b), fill voids in remotely sensed XCO_2 surfaces (Yue et al., 2015a), and to analyze ecosystem responses to climatic change (Yue et al., 2015b). In all of these applications, HASM produced more accurate results than the classical methods (Yue et al., 2015c).

3.6 Estimation of carbon stocks

Forest carbon stocks and carbon densities were estimated by methods of spatial interpolation, SOA, LPJ, data fusion and data assimilation. The spatial interpolation provided an effective approach to construct a continuous surface from the FID by means of Kriging; it took advantage of limited observation data to estimate the most plausible spatial distribution by filling in missing data. The data fusion approach integrated the forest inventory and satellite data into a consistent, accurate and useful representation using HASM (HASM-SOA); the aim of the data fusion was to improve the quality of the information so that it was more accurate than would be possible if the data sources had been used individually. The data assimilation incorporated FID into LPJ by means of HASM (HASM-LPJ); the aim of the data assimilation was to derive accurate estimates of the current and future states of the forest carbon stocks in China.

BGD
12, 19535–19577, 2015

3.7 Validation

The uncertainties of the carbon stock estimates reported in earlier studies relied on several different concepts and metrics. The same formula for absolute and relative error should be used to evaluate all estimates of carbon stocks so that the estimation results are comparable. We calculated the mean absolute errors (MAE) and mean relative errors (MRE), respectively, as:

$$\mathrm{MAE} = \frac{1}{n}\sum_{i}^{n}|o_i - s_i| \tag{6}$$

$$\mathrm{MRE} = \frac{\mathrm{MAE}}{\frac{1}{n}\sum_{i}^{n}|o_i|} \tag{7}$$

where o_i represents the forest carbon stocks at the ith control point; s_i represents the simulated value at the ith control point; and n_i is the total number of control points used for validation.

Cross-validation was comprised of four steps: (1) 5 % of the sample plots from the national forest inventory were removed for validation; (2) the spatial distribution of average forest CSs in China during the period 2004–2008 were simulated at a spatial resolution of 5 km × 5 km using the remaining 95 % of the sample plots from the national forest inventory by means of the different methods; (3) the MAEs and MREs were calculated using the 5 % validation set; and (4) the 5 % validation set was returned to the pool for the next iteration, and another 5 % validation set was removed. This final process was repeated until the all sample plots were used for validation at least one time and the simulation error statistics could be calculated for each sample plot.

BGD
12, 19535–19577, 2015

4 Results

The five maps of forest biomass mean annual carbon stocks during the period 2004–2008 reproduced with each of the aforementioned methods shows how each of the methods was able to generate the same overall patterns based on the underlying forest cover on the one hand, and how the estimates varied using each of these methods over large parts of the China on the other hand (Fig. 2). This variability raises questions related to the reliability of the estimates produced with the five aforementioned approaches.

The cross-validation results indicated that LPJ, Kriging and SOA had larger errors, with MREs of 79.33, 50.12 and 48.77 %, respectively. LPJ and Kriging over-estimated the carbon stocks, while SOA under-estimated the carbon stocks (Table 4). Accuracy was considerably improved when the forest inventory and satellite data were fused by using HASM-SOA and the mechanism-based model was combined with the FID by using HASM-LPJ. The MREs of HASM-SOA and HASM-LPJ were 22.71 and 31.26 %, respectively.

The mean annual carbon stocks (MACSs) of all forest types estimated with HASM-SOA (the best approach) was 7.08 Pg in China during the period 2004–2008. The MACSs of coniferous, broadleaf and mixed forests were 2.74, 3.95 and 0.39 Pg, respectively (Table 5). The mean annual carbon densities (MACDs) of the coniferous, broadleaf and mixed forests were 4.35, 4.74 and 4.20 kg m^{-2}, respectively.

The land mass of China was next divided into nine regions (Fig. 3) with similar temperature, precipitation and soil regimes to make it easier to analyze changes in forest carbon storage from one place to another (Zhou et al., 1981). The nine regions are referred to as Ri where $i = 1$ to 9 and we use P1, P2, P3, P4 and P5 to represent the periods 1984–1988, 1989–1993, 1994–1998, 1999–2003 and 2004–2008, respectively.

The HASM-SOA estimates showed that 89.9 % of the MACSs were found in the regions R5, R3, R6, R9 and R7 during the period P5, accounting for 28.61, 28.41,

BGD
12, 19535–19577, 2015

Modeling the uncertainty of estimating forest carbon stocks in China

T. X. Yue et al.

14.48, 12.52 and 5.89 % of the MACSs, respectively. The three largest MACDs occurred in R5 (Tibet plateau; 10.53 $kg\,m^{-2}$), R2 (arid area; 6.33 $kg\,m^{-2}$) and R3 (northeastern China; 4.44 $kg\,m^{-2}$) (Table 6 and Fig. 2e). The two smallest MACDs were predicted in the R8 (2.14 $kg\,m^{-2}$) and R9 (2.60 $kg\,m^{-2}$) regions.

The HASM-SOA estimates can be parsed by forest type as well (Table 7). Hence, the MACDs of evergreen broad-leaved and evergreen coniferous forests were 6.23 and 4.47 $kg\,m^{-2}$, respectively, while the MACDs for deciduous broad-leaved and deciduous coniferous forests were 3.93 and 3.77 $kg\,m^{-2}$, respectively in P5. The MACD of evergreen forests was 50 % larger than that of deciduous forests, and the MACDs for broad-leaved forests were greater than those for both coniferous and deciduous forests. Turning next to the MACSs, the evergreen coniferous forests contributed the largest proportion, accounting for 33.05 %, followed by deciduous broad-leaved forests (29.8 %), and evergreen broad-leaved forests (25.99 %). The deciduous coniferous and the broad-leaved and coniferous mixed forests accounted for the first two smallest proportions of the total MACS, 5.65 and 5.51 %, respectively.

The HASM-SOA estimates also indicate that MACSs rose from 4.84 Pg in P1 to 7.08 Pg in P5 due to the increase of MACD and the expansion of forest area (Table 8). The MACD rose from 4.00 $kg\,m^{-2}$ in P1 to 4.55 $kg\,m^{-2}$ in P5 and the forest area grew from 1.21 million km^2 in P1 to 1.56 million km^2 in P5. The increasing trends of the MACS, MACD and forest area (FA) are captured by the following regression equations:

$$\mathrm{MACS}(t) = 0.531t + 4.297\,, \qquad R = 0.976 \tag{8}$$

$$\mathrm{MACD}(t) = 0.125t + 3.958\,, \qquad R = 0.943 \tag{9}$$

$$\mathrm{FA}(t) = 0.083t + 1.1045\,, \qquad R = 0.96 \tag{10}$$

where t corresponds to Pt, $t = 1$, 2, 3, 4 and 5; MACS(t), MACD(t) and FA(t) are MACS, MACD and FA, respectively in the period Pt; and R represents the correlation coefficient for the corresponding regression equation.

Although MACS rose in all nine regions from P1 to P5, the spatial variability over China more or less mirrors the variability in the distribution of forests (Fig. 4, Table 9).

For regions R1 and R8, for example, both MACS and MACD have continuously increased from P1 to P5. R8 has the smallest MACS, which only accounted for 0.83 % of the MACS of the whole of China, and the smallest MACD of 2.14 $\mathrm{kg\,m^{-2}}$ in P5 as well as the lowest CS accumulation rate of 1.3 $\mathrm{Tg\,yr^{-1}}$. In R1, MACS accounted for 3.94 % of the total MACS of China for the period of P5 and the CS accumulation rate has averaged 6.2 $\mathrm{Tg\,yr^{-1}}$ from P1 to P5.

The region R5 had the largest MACS accounting for 28.61 % of the total MACS of China in P5, the largest MACD of 10.53 $\mathrm{kg\,m^{-2}}$ and the fastest CS accumulation rate of 52 $\mathrm{Tg\,yr^{-1}}$; the MACS has shown a monotonically increasing trend since P1. The second largest MACS occurred in R3 (Northeastern China). The MACS in R3 accounted for 28.41 % of the total MACS of China. However, the MACD in R3 has declined since P3 following increases from P1 to P2 and from P2 to P3. The mean CS accumulation rate in R3 was 21.3 $\mathrm{Tg\,yr^{-1}}$.

In the regions R4 (Loess Plateau), R6 and R9, both MACS and MACD have increased since P3. The MACSs in R4, R6 and R9 accounted for 2.68, 14.48 and 12.26 % of the MACS in the whole of China in P5, respectively. The average CS accumulation rates were 2.8, 10.4 and 12.7 $\mathrm{Tg\,yr^{-1}}$, respectively in R4, R6, and R9. In R2 (an arid area of China), the MACS accounted for 2.80 % of the total for China in the period P5. The MACS and MACD increased from P4 to P5, but the mean accumulation rate of CS was only 2.3 $\mathrm{Tg\,yr^{-1}}$. The MACS accounted for 5.89 % of the total for China in R7. The MACS and MACD both increased from P4 to P5 but like in R2, the mean CS accumulation rate was relatively low at just 2.9 $\mathrm{Pg\,yr^{-1}}$.

In terms of forest types, evergreen broad-leaved forests had the fastest CS accumulation rate and the largest MACD, while evergreen coniferous forests contributed the largest MACS. The MACSs of broad-leaved forests increased during all five periods. The MACS of evergreen broad-leaved forests increased from 0.63 Pg in period P1 to 1.84 Pg in P5, and the MACSs for deciduous broad-leaved forests rose from 1.38 Pg in P1 to 2.11 Pg in P5. These trends can be modeled with the following

BGD
12, 19535–19577, 2015

regression equations:

$$\mathrm{MACS}_1(t) = 0.312t + 0.286\,, \qquad R = 0.998 \tag{11}$$

$$\mathrm{MACS}_2(t) = 0.199t + 1.115\,, \qquad R = 0.981 \tag{12}$$

where t corresponds to Pt, $t = 1$, 2, 3, 4 and 5; $\mathrm{MACS}_1(t)$ and $\mathrm{MACS}_2(t)$ are respectively the MACSs of evergreen broad-leaved forests and deciduous broad-leaved forests in the period Pt and R represents correlation coefficient of the corresponding regression equation.

The MACSs of deciduous coniferous forests fluctuated from period to period. Evergreen coniferous forests and broad-leaved and coniferous mixed forests exhibited an increasing trend of MACS in general but declined P3. Their trends were modeled with the following regression equations:

$$\mathrm{MACS}_3(t) = 0.207t + 1.391\,, \qquad R = 0.932 \tag{13}$$

$$\mathrm{MACS}_4(t) = 0.076t - 0.068\,, \qquad R = 0.867 \tag{14}$$

where t corresponds to Pt, $t = 1$, 2, 3, 4 and 5; $\mathrm{MACS}_3(t)$ represents the MACSs of evergreen coniferous forests in the period Pt; $\mathrm{MACS}_4(t)$ refers to the broad-leaved and coniferous mixed forests; and R represents correlation coefficient of the corresponding regression equation.

5 Discussion and conclusions

The ground-based national forest inventory is able to accurately estimate forest carbon stocks with high temporal resolution at sample plots, but these sample plots are too sparse to support spatial simulation of carbon stocks with high accuracy. Satellite remote-sensing can supply spatially continuous information about the surface of forest carbon stocks, which cannot be obtained from ground-based investigations, but these remote sensing descriptions contain considerable uncertainty. The fusion of forest inventory data with satellite observations achieved with HASM-SOA provided much more accurate estimates of forest biomass carbon stocks and their changes. This kind of method can increase our understanding of the role of forests in the carbon cycle, for greenhouse gas inventories, and terrestrial carbon accounting (Muukkonen and Heiskanen, 2007).

Turning to the work at hand, HASM-SOA overcame the shortcomings of both the ground-based national forest inventory and the satellite remote-sensing observations by fusing information about the details of the carbon stocks observed on the Earth's surface and the variability of the carbon surface observed from space. The cross-validation demonstrated that HASM-SOA was 26.1 % more accurate than the satellite-based approach and 28.4 % more accurate than spatial interpolation of the sample plots. These findings suggest that China's forest biomass carbon stocks are more likely to match our estimates than those generated by past efforts to estimate these same carbon stocks and their change over time.

Taken as a whole, the HASM-SOA results show that the forest carbon stocks of China have increased by 2.24 Pg during the period 1984–2008 to a new high of 7.08 Pg C in 2008. These numbers fall in the middle of the previously published estimates. All of the estimates show forest biomass carbon stocks in China increasing from 1973 to 2008, notwithstanding the various methods used and the varying levels of uncertainty embedded in these different methods and the data sources used.

Acknowledgements. This work is supported by National Natural Science Foundation of China (91325204), by National High-tech R&D Program of the Ministry of Science and Technology of the People's Republic of China (2013AA122003), and by National Basic Research Priorities Program (2010CB950904) of Ministry of Science and Technology of the People's Republic of China.

BGD
12, 19535–19577, 2015

References

Ahlstroem, A., Schurgers, G., Arneth, A., and Smith, B.: Robustness and uncertainty in terrestrial ecosystem carbon response to CMIP5 climate change projections, Environ. Res. Lett., 7, 044008, doi:10.1088/1748-9326/7/4/044008, 2012.

Alvarez, E., Duque, A., Saldarriaga, J., Cabrera, K., de las Salas, G., del Valle, I., Lema, A., Moreno, F., Orrego, S., and Rodriguez, L.: Tree above-ground biomass allometries for carbon stocks estimation in the natural forests of Colombia, Forest Ecol. Manag., 267, 297–308, 2012.

Apps, M. J., Kurz, W. A., Luxmoore, R. J., Nilsson, L. O., Sedjo, R. A., Schmidt, R., Simpson, L. G., and Vinson, T. S.: Boreal forests and tundra, Water Air Soil Poll., 70, 39–53, 1993.

Barman, R., Jain, A. K., and Liang, M. L.: Climate-driven uncertainties in modeling terrestrial gross primary production: a site level to global-scale analysis, Glob. Change Biol., 20, 1394–1411, 2014.

Bradshaw, C. J. A. and Warkentin, I. G.: Global estimates of boreal forest carbon stocks and flux, Global Planet. Change, 128, 24–30, 2015.

Brovkin, V., Ganopolski, A., and Svirezhev, Y.: A continuous climate–vegetation classification for use in climate–biosphere studies, Ecol. Model., 101, 251–261, 1997.

Butt, N., Epps, K., Overman, H., Iwamura, T., and Fragoso, J. M. V.: Assessing carbon stocks using indigenous peoples' field measurements in Amazonian Guyana, Forest Ecol. Manag., 338, 191–199, 2015.

Canadell, J. G. and Raupach, M. R.: Managing forests for climate change mitigation, Science, 320, 1456–457, 2008.

Chave, J., Andalo, C., Brown, S., Cairns, M. A., Chambers, J. Q., Eamus, D., Folster, H., Fromard, F., Higuchi, N., Kira, T., Lescure, J. P., Nelson, B. W., Ogawa, H., Puig, H., Riéra, B., and Yamakura, T.: Tree allometry and improved estimation of carbon stocks and balance in tropical forests, Oecologia, 145, 87–99, 2005.

Chen, C. F. and Yue, T. X.: A method of DEM construction and related error analysis, Comput. Geosci., 36, 717–725, 2010.

Chen, C. F., Yue, T. X., Dai, H. L., and Tian, M. Y.: The smoothness of HASM, Int. J. Geogr. Inf. Sci., 27, 1651–1667, 2013a.

Chen, C. F., Li, Y. Y., and Yue, T. X.: Surface modeling of DEMs based on a sequential adjustment method, Int. J. Geogr. Inf. Sci., 27, 1272–1291, 2013b.
Chen, J. M., Ju, W., Cihlar, J., Price, D., Liu, J., Chen, W., Pan, J., Black, A., and Barr, A.: Spatial distribution of carbon sources and sinks in Canada's forests, Tellus B, 55, 622–641, 2003.
Chiesi, M., Maselli, F., Moriondo, M., Fibbi, L., Bindi, M., and Running, S. W.: Application of BIOME-BGC to simulate Mediterranean forest processes, Ecol. Model., 206, 179–190, 2007.
Cramer, W., Bondeau, A., and Woodward, F. I.: Global response of terrestrial ecosystem structure and function to CO_2 and climate change: results from six dynamic global vegetation models, Glob. Change Biol., 7, 357–373, 2001.
Daly, C., Bachelet, D., Lenihan, J. M., Neilson, R. P., Parton, W., and Ojima, D.: Dynamic simulation of tree-grass interactions for global change studies, Ecol. Appl., 10, 449–469, 2000.
Deng, S. H., Shi, Y. Q., Jin, Y., and Wang, L. H.: A GIS-based approach for quantifying and mapping carbon sink and stock values of forest ecosystem: a case study, Energy Procedia, 5, 1535–1545, 2011.
Domke, G. M., Woodall, C. W., Smith, J. E., Westfall, J. A., and McRoberts, R. E.: Consequences of alternative tree-level biomass estimation procedures on U. S. forest carbon stock estimates, Forest Ecol. Manag., 270, 108–116, 2012.
Dybzinski, R., Farrior, C., Wolf, A., Reich, P. B., and Pacala, S. W.: Evolutionarily stable strategy carbon allocation to foliage, wood, and fine roots in trees competing for light and nitrogen: an analytically tractable, individual-based model and quantitative comparisons to data, Am. Nat., 177, 153–166, 2011.
Dybzinski, R., Farrior, C. E., Ollinger, S., and Pacala, S. W.: Interspecific vs. intraspecific patterns in leaf nitrogen of forest trees across nitrogen availability gradients, New Phytol., 200, 112–121, 2013.
Dybzinski, R., Farrior, C. E., and Pacala, S. W.: Increased forest carbon storage with increased atmospheric CO_2 despite nitrogen limitation: a game-theoretic allocation model for trees in competition for nitrogen and light, Glob. Change Biol., 21, 1182–1196, 2015.
Editorial Board of Vegetation Map of China: Vegetation Atlas of China, Science Press, Beijing, 2001 (in Chinese).
Fang, J. Y., Guo, Z. D., Piao, S. L., and Chen, A. P.: Terrestrial vegetation carbon sinks in China, 1981–2000, Sci. China Ser. D, 50, 1341–1350, 2007.

Farrior, C. E., Dybzinski, R., Levin, S. A., and Pacala, S. W.: Competition for water and light in closed-canopy forests: a tractable model of carbon allocation with implications for carbon sinks, Am. Nat., 181, 314–330, 2013.

Flores, O. and Coomes, D. A.: Estimating the wood density of species for carbon stock assessments, Methods in Ecology and Evolution, 2, 214–220, 2011.

Foley, J. A., Prentice, I. C., Ramankutty, N., Levis, S., Pollard, D., Sitch, S., and Haxeltine, A.: An integrated biosphere model of land surface processes, terrestrial carbon balance, and vegetation dynamics, Global Biogeochem. Cy., 10, 603–628, 1996.

Franklin, O., Johansson, J., Dewar, R. C., Dieckmann, U., McMurtrie, R. E., Brannstrom, A., and Dybzinski, R.: Modeling carbon allocation in trees: a search for principles, Tree Physiol., 32, 648–666, 2012.

Friend, A. D., Stevens, A. K., Knox, R. G., and Cannell, M. G. R.: A process-based terrestrial biosphere model of ecosystem dynamics (Hybrid v3.0), Ecol. Model., 95, 249–287, 1995.

Gao, Z. Q. and Liu, J. Y.: Simulation study of China's net primary production, Chinese Sci. Bull., 53, 434–443, 2008.

Gonzalez-Benecke, C. A., Martin, T. A., Cropper Jr, W. P., and Bracho, R.: Forest management effects on in situ and ex situ slash pine forest carbon balance, Forest Ecol. Manag., 260, 795–805, 2010.

Guo, Z. D., Fang, J. Y., Pan, Y. D., and Birdsey, R.: Inventory-based estimates of forest biomass carbon stocks in China: a comparison of three methods, Forest Ecol. Manag., 259, 1225–1231, 2010.

Heo, J., Kim, J. W., Pattnaik, S., and Sohn, H. G.: Quality improvement of loblolly pine (*Pinus taeda*) plantation inventory GIS using Shuttle Radar Topography Mission (STRM) and the National Elevation Dataset (NED), Forest Ecol. Manag., 233, 61–68, 2006.

Hidy, D., Barcza, Z., Haszpra, L., Churkina, G., Pintér, K., and Nagy, Z.: Development of the Biome-BGC model for simulation of managed herbaceous ecosystems, Ecol. Model., 226, 99–119, 2012.

Holdaway, R. J., McNeill, S. J., Mason, N. W. H., and Carswell, F. E.: Propagating uncertainty in plot-based estimates of forest carbon stock and carbon stock change, Ecosystems, 17, 627–640, 2014.

Hyyppa, J., Hyyppa, H., Inkinen, M., Engdahl, M., Linko, S., and Zhu, Y. H.: Accuracy comparison of various remote sensing data sources in the retrieval of forest stand attributes, Forest Ecol. Manag., 128, 109–120, 2000.

BGD
12, 19535–19577, 2015

Modeling the uncertainty of estimating forest carbon stocks in China

T. X. Yue et al.

Jung, J., Kim, S., Hong, S., Kim, K., Kim, E., Im, J., and Heo, J.: Effects of national forest inventory plot location error on forest carbon stock estimation using k-nearest neighbor algorithm, ISPRS J. Photogramm., 81, 82–92, 2013.
Karna, Y. K., Hussin, Y. A., Gilani, H., Bronsvel, M. C., Murthy, M. S. R., Qamer, F. M., Karky, B. S., Bhattarai, T., Xu, A. G., and Baniya, C. B.: Integration of WorldView-2 and airborne LiDAR data for tree species level carbon stock mapping in Kayar Khola watershed, Nepal, Int. J. Appl. Earth Obs., 38, 280–291, 2015.
Kearsley, E., de Haulleville, T., Hufkens, K., Kidimbu, A., Toirambe, B., Baert, G., Huygens, D., Kebede, Y., Defourny, P., Bogaert, J., Beeckman, H., Steppe, K., Boeckx, P., and Verbeeck, H.: Conventional tree height–diameter relationships significantly overestimate aboveground carbon stocks in the Central Congo Basin, Nature Communications, 4, 2269, doi:10.1038/ncomms3269, 2013.
Kucharik, C. J., Foley, J. A., Delire, C., Fisher, V. A., Coe, M. T., Lenters, J. D., Young-Molling, C., Ramankutty, N., Norman, J. M., and Gower, S. T.: Testing the performance of a Dynamic Global Ecosystem Model: water balance, carbon balance, and vegetation structure, Global Biogeochem. Cy., 14, 795–825, 2000.
Kurz, W. A., Dymond, C. C., White, T. M., Stinson, G., Shaw, C. H., Rampley, G. J., Smyth, C., Simpson, B. N., Neilson, E. T., Trofymow, J. A., Metsaranta, J., and Apps, M. J.: CBM-CFS3: a model of carbon-dynamics in forestry and land-use change implementing IPCC standards, Ecol. Model., 220, 480–504, 2009.
Landsberg, J. J. and Waring, R. H.: A generalised model of forest productivity using simplified concepts of radiation-use efficiency, carbon balance and partitioning, Forest Ecol. Manag., 95, 209–228, 1997.
Li, H. K. and Lei, Y. C.: Estimation and Evaluation of Forest Biomass Carbon Storage in China, China Forestry Press, Beijing, 2010 (in Chinese).
Liski, J., Karjalainen, T., Pussinen, A., Nabuurs, G. J., and Kauppi, P.: Trees as carbon sinks and sources in the European Union, Environ. Sci. Policy, 3, 91–97, 2000.
Liu, J., Chen, J. M., Cihlar, J., and Chen, W.: Net primary productivity mapped for Canada at 1 km resolution, Global Ecol. Biogeogr., 11, 115–129, 2002.
McMurtrie, R. E. and Dewar, R. C.: New insights into carbon allocation by trees from the hypothesis that annual wood production is maximized, New Phytol., 199, 981–990, 2013.

BGD
12, 19535–19577, 2015
Modeling the uncertainty of estimating forest carbon stocks in China
T. X. Yue et al.

Medvigy, D., Wofsy, S. C., Munger, J. W., Hollinger, D. Y., and Moorcroft, P. R.: Mechanistic scaling of ecosystem function and dynamics in space and time: Ecosystem Demography model version 2, J. Geophys. Res., 114, G01002, doi:10.1029/2008JG000812, 2009.

Moorcroft, P. R., Hurtt, G. C., and Pacala, S. W.: A method for scaling vegetation dynamics: the ecosystem demography model (ED), Ecol. Monogr., 71, 557–586, 2001.

Muukkonen, P. and Heiskanen, J.: Biomass estimation over a large area based on standwise forest inventory data and ASTER and MODIS satellite data: a possibility to verify carbon inventories, Remote Sens. Environ., 107, 617–624, 2007.

Navar, J.: Allometric equations for tree species and carbon stocks for forests of northwestern Mexico, Forest Ecol. Manag., 257, 427–434, 2009.

Ni, J.: Carbon storage in Chinese terrestrial ecosystems: approaching a more accurate estimate, Climatic Change, 119, 905–917, 2013.

Pan, Y., Birdsey, R. A., Fang, J. Y., Houghton, R., Kauppi, P. E., Kurz, W. A., Phillips, O. L., Shvidenko, A., Lewis, S. M., Canadell, J. G., Ciais, P., Jackson, R. B., Pacala, S. W., McGuire, A. D., Piao, S. L., Rautiainen, A., Sitch, S., and Hayes, D.: A large and persistent carbon sink in the world's forests, Science, 333, 988–993, 2011.

Patenaude, G., Milne, R., and Dawson, T. P.: Synthesis of remote sensing approaches for forest carbon estimation: reporting to the Kyoto Protocol, Environ. Sci. Policy, 8, 161–178, 2005.

Petrokofsky, G., Kanamaru, H., Achard, F., Goetz, S. J., Joosten, H., Holmgren, P., Lehtonen, A., Menton, M. C. S., Pullin, A. S., and Wattenbach, M.: Comparison of methods for measuring and assessing carbon stocks and carbon stock changes in terrestrial carbon pools: how do the accuracy and precision of current methods compare? A systematic review protocol, Environmental Evidence, 1, 2–21, 2012.

Piao, S. L., Fang, J. Y., Zhu, B., and Tan, K.: Forest biomass carbon stocks in China over the past 2 decades: estimation based on integrated inventory and satellite data, J. Geophys. Res., 110, G01006, doi:10.1029/2005JG000014, 2005.

Piao, S. L., Fang, J. Y., Ciais, P., Peylin, P., Huang, Y., Sitch, S., and Wang, T.: The carbon balance of terrestrial ecosystems in China, Nature, 458, 1009–1014, 2009.

Potter, C., Klooster, S., Crabtree, R., Huang, S. L., Gross, P., and Genovese, V.: Carbon fluxes in ecosystems of Yellowstone National Park predicted from remote sensing data and simulation modeling, Carbon Balance and Management, 6, 16 pp., doi:10.1186/1750-0680-6-3, 2011.

BGD
12, 19535–19577, 2015

Potter, C. S., Ranserson, J. T., Field, C. B., Matson, P. A., Vitousek, P. M., Mooney, H. A., and Klooster, S. A.: Terrestrial ecosystem production: a process model based on globe satellite and surface data, Global Biogeochem. Cy., 7, 811–842, 1993.

Prentice, I. C., Farquhar, G. D., Fasham, M. J. R., Goulden, M. L., Heimann, M., Jaramillo, V. J., Kheshgi, H. S., Le Quere, C., Scholes, R. J., Wallace, D. W. R., Archer, D., Ashmore, M. R., Aumont, O., Baker, D., Battle, M., Bender, M., Bopp, L. P., Bousquet, P., Caldeira, K., Ciais, P., Cox, P. M., Cramer, W., Dentener, F., Enting, I. G., Field, C. B., Friedlingstein, P., Holland, E. A., Houghton, R. A., House, J. I., Ishida, A., Jain, A. K., Janssens, I. A., Joos, F., Kaminski, T., Keeling, C. D., Keeling, R. F., Kicklighter, D. W., Hohfeld, K. E., Knorr, W., Law, R., Lenton, T., Lindsay, K., Maier-Reimer, E., Manning, A. C., Matear, R. J., McGuire, A. D., Melillo, J. M., Meyer, R., Mund, M., Orr, J. C., Piper, S., Plattner, K., Rayner, P. J., Sitch, S., Slater, R., Taguchi, S., Tans, P. P., Tian, H. Q., Weirig, M. F., Whorf, T., and Yool, A.: The carbon cycle and atmospheric carbon dioxide, in: Climate Change 2001: The Scientific Basis, edited by: Houghton, J. T., Ding, Y., Griggs, D. J., Noguer, M., Van Der Linden, P. J., Dai, X., Maskell, K., Johnson, C. A., Cambridge University Press, Cambridge, 183–237, 2001.

Prince, S. D. and Goward, S. N.: Global primary production: a remote sensing approach, J. Biogeogr., 22, 815–835, 1995.

Running, S. W. and Coughlan, J. C.: A general model of forest ecosystem processes for regional applications: I, Hydrologic balance, canopy gas exchange and primary processes, Ecol. Model., 42, 125–154, 1988.

Schmid, S., Zierl, B., and Bugmann, H.: Analyzing the carbon dynamics of central European forests: comparison of Biome-BGC simulations with measurements, Reg. Environ. Change, 6, 167–180, 2006.

Shaw, C. H., Hilger, A. B., Metsaranta, J., Kurz, W. A., Russo, G., Eichel, F., Stinson, G., Smyth, C., and Filiatrault, M.: Evaluation of simulated estimates of forest ecosystem carbon stocks using ground plot data from Canada's National Forest Inventory, Ecol. Model., 272, 323–347, 2014.

Shi, W. J., Liu, J. Y., Song, Y. J., Du, Z. P., Chen, C. F., and Yue, T. X.: Surface modeling of soil pH, Geoderma, 150, 113–119, 2009.

Shi, W. J., Liu, J. Y., Du, Z. P., Stein, A., and Yue, T. X.: Surface modeling of soil properties based on land use information, Geoderma, 162, 347–357, 2011.

Sierra, C. A., del Valle, J. I., Orrego, S. A., Moreno, F. H., Harmon, M. E., Zapata, M., Colorado, G. J., Herrera, M., Lara, W., Restrepo, D. E., Berrouet, L. M., Loaiza, L. M., and Benjumea, J. F.: Total carbon stocks in a tropical forest landscape of the Porce region, Colombia, Forest Ecol. Manag., 243, 299–309, 2007.

Singh, R. P., Rovshan, S., Goroshi, S. K., Panigrahy, S., and Parihar, J. S.: Spatial and temporal variability of net primary productivity (NPP) over terrestrial biosphere of India using NOAA-AVHRR based GloPEM model, Journal of the Indian Society of Remote Sensing, 39, 345–353, 2011.

Sitch, S., Smith, B., Prentice, I. C., Arneth, A., Bondeau, A., Cramer, W., Kaplan, J. O., Levis, S., Lucht, W., Sykes, M. T., Thonicke, K., and Venevsky, S.: Evaluation of ecosystem dynamics, plant geography and terrestrial carbon cycling in the LPJ Dynamic Global Vegetation Model, Glob. Change Biol., 9, 161–185, 2003.

Strand, E. K., Vierling, L. A., Smith, A. M. S., and Bunting, S. C.: Net changes in aboveground woody carbon stock in western juniper woodlands, 1946–1998, J. Geophys. Res., 113, G01013, doi:10.1029/2007JG000544, 2008.

Stuemer, W., Kenter, B., and Koehl, M.: Spatial interpolation of in situ data by self-organizing map algorithms (neural networks) for the assessment of carbon stocks in European forests, Forest Ecol. Manag., 260, 287–293, 2010.

Thurner, M., Beer, C., Santoro, M., Carvalhais, N., Wutzler, T., Schepaschenko, D., Shvidenko, A., Kompter, E., Ahrens, B., Levick, S. R., and Schmullius, C.: Carbon stock and density of northern boreal and temperate forests, Global Ecol. Biogeogr., 23, 297–310, 2014.

Tomppo, E. and Halme, M.: Using coarse scale forest variables as ancillary information and weighting of variables in k-NN estimation: a genetic algorithm approach, Remote Sens. Environ., 92, 1–20, 2004.

van Breugel, M., Ransijn, J., Craven, D., Bongers, F., and Hall, J. S.: Estimating carbon stock in secondary forests: decisions and uncertainties associated with allometric biomass models, Forest Ecol. Manag., 262, 1648–1657, 2011.

Venevsky, S. and Maksyutov, S.: SEVER: a modification of the LPJ global dynamic vegetation model for daily time step and parallel computation, Environ. Modell. Softw., 22, 104–109, 2007.

Wang, S., Chen, J. M., Ju, W. M., Feng, X., Chen, M., Chen, P., and Yu, G.: Carbon sinks and sources in China's forests during 1901–2001, J. Environ. Manage., 85, 524–537, 2007.

Woodward, F. I., Lomas, M. R., and Betts, R. A.: Vegetation-climate feedbacks in a greenhouse world, Philos. T. Roy. Soc. B, 353, 29–38, 1998.
Xu, Z. G., Xu, J. T., Deng, X. Z., Huang, J. K., Uchida, E., and Rozelle, S.: Grain for Green versus grain: conflict between food security and conservation set-aside in China, World Dev., 34, 130–148, 2006.
Yang, K. and Guan, D. S.: Changes in forest biomass carbon stock in the Pearl River Delta between 1989 and 2003, J. Environ. Sci., 20, 1439–1444, 2008.
Yu, G. R., Chen, Z., Piao, S. L., Peng, C. H., Ciais, P., Wang, Q. F., Li, X. R., and Zhu, X. J.: High carbon dioxide uptake by subtropical forest ecosystems in the East Asian monsoon region, P. Natl. Acad. Sci. USA, 111, 4910–4915, 2014.
Yuan, W. P., Liu, S. G., Zhou, G. S., Zhou, G. Y., Tieszen, L. L., Baldocchi, D., Bernhofer, C., Gholz, H., Goldstein, A. H., Goulden, M. L., Hollinger, D. Y., Hu, Y., Law, B. E., Stoy, P. C., Vesala, T., and Wofsy, S. C.: Deriving a light use efficiency model from eddy covariance flux data for predicting daily gross primary production across biomes, Agr. Forest Meteorol., 143, 189–207, 2007.
Yue, T. X.: Surface Modelling: High Accuracy and High Speed Methods, CRC Press, Boca Raton, FL, 2011.
Yue, T. X. and Wang, S. H.: Adjustment computation of HASM: a high-accuracy and high-speed method, Int. J. Geogr. Inf. Sci., 24, 1725–1743, 2010.
Yue, T. X., Du, Z. P., Song, D. J., and Gong, Y.: A new method of surface modeling and its application to DEM construction, Geomorphology, 91, 161–172, 2007.
Yue, T. X., Chen, C. F., and Li, B. L.: An adaptive method of high accuracy surface modeling and its application to simulating elevation surfaces, Transactions in GIS, 14, 615–630, 2010a.
Yue, T. X., Song, D. J., Du, Z. P., and Wang, W.: High-accuracy surface modelling and its application to DEM generation, Int. J. Remote Sens., 31, 2205–2226, 2010b.
Yue, T. X., Wang, Q., Lu, Y. M., Xin, X. P., Zhang, H. B., and Wu, S. X.: Change trends of food provisions in China, Global Planet. Change, 72, 118–130, 2010c.
Yue, T. X., Chen, C. F., and Li, B. L.: A high accuracy method for filling SRTM voids and its verification, Int. J. Remote Sens., 33, 2815–2830, 2012.
Yue, T. X., Zhao, N., Yang, H., Song, Y. J., Du, Z. P., Fan, Z. M., and Song, D. J.: The multi-grid method of high accuracy surface modelling and its validation, Transactions in GIS, 17, 943–952, 2013a.

Yue, T. X., Zhao, N., Ramsey, R. D., Wang, C. L., Fan, Z. M., Chen, C. F., Lu, Y. M., and Li, B. L.: Climate change trend in China, with improved accuracy, Climatic Change, 120, 137–151, 2013b.

Yue, T. X., Du, Z. P., Lu, M., Fan, Z. M., Wang, C. L., Tian, Y. Z., and Xu, B.: Surface modelling of ecosystem responses to climatic change, Ecol. Model., 306, 16–23, 2015a.

Yue, T. X., Zhao, M. W., and Zhang, X. Y.: A high-accuracy method for filling voids on remotely sensed XCO_2 surfaces and its verification, J. Clean. Prod., 103, 819–827, 2015b.

Yue, T. X., Zhang, L. L., Zhao, N., Zhao, M. W., Chen, C. F., Du, Z. P., Song, D. J., Fan, Z. M., Shi, W. J., Wang, S. H., Yan, C. Q., Li, Q. Q., Sun, X. F., Yang, H., Wang, C. L., Wang, Y. F., Wilson, J. P., and Xu, B.: A review of recent developments in HASM, Environmental Earth Sciences, 74, 6541–6549, 2015c.

Zhang, C. H., Ju, W. M., Chen, J. M., Zan, M., Li, D. Q., Zhou, Y. L., and Wang, X. Q.: China's forest biomass carbon sink based on seven inventories from 1973 to 2008, Climatic Change, 118, 933–948, 2013.

Zhao, M. F., Xiang, W. H., Peng, C. H., and Tian, D. L.: Simulating age-related changes in carbon storage and allocation in a Chinese fir plantation growing in southern China using the 3-PG model, Forest Ecol. Manag., 257, 1520–1531, 2009.

Zhao, N. and Yue, T. X.: A modification of HASM for interpolating precipitation in China, Theor. Appl. Climatol., 116, 273–285, 2014a.

Zhao, N. and Yue, T. X.: Sensitivity studies of a high accuracy surface modelling method, Sci. China Ser. D, 57, 1–11, 2014b.

Zhou, L. S., Sun, H., Shen, Y. Q., Deng, J. Z., Shi, Y. L.: Comprehensive Agricultural Planning of China, China Agricultural Press, Beijing, 1981 (in Chinese).

Table 1. Converted farmland and reforested bare land included in China's Grain for Green Program (millions ha).

Year	Converted farmland	Afforestation on bare land	Total
1999	0.381	0.066	0.448
2000	0.405	0.468	0.872
2001	0.42	0.563	0.983
2002	2.647	3.082	5.729
2003	3.367	3.767	7.133
2004	0.667	3.333	4
2005	1.114	1.321	2.435
2006–2010	5.666	4.733	10.4
2014	0.333		0.333
2015	0.667		0.667
1999–2015	15.667	17.333	33
2016–2020	1.827		1.827

BGD
12, 19535–19577, 2015
Modeling the uncertainty of estimating forest carbon stocks in China
T. X. Yue et al.

Table 2. Parameters used to calculate BEFs in China (Fang et al., 2007).

Forest type	a ($kg\,m^{-3}$)	b ($kg\,m^{-2}$)	Number of samples	R^2
Abies, Picea	551.9	4.8861	24	0.78
Tsuga, Cryptomeria, Keteleeria	349.1	3.9816	30	0.79
Larix	609.6	3.3806	34	0.82
P. koraiensis	572.3	1.6489	22	0.93
P. sylyestris var. mongolica	1112	0.2695	15	0.85
P. tabulaefomis	869	0.9121	112	0.91
P. armandii	585.6	1.8744	9	0.91
P. massoniana, P. yunnanensis	503.4	2.0547	52	0.87
Cunninghamialanceolata	465.2	1.9141	90	0.94
Cypress	889.3	0.7397	19	0.87
Other pines and conifer forests	529.2	2.5087	19	0.86
Deciduous oaks	1145.3	0.8547	12	0.98
Betula	1068.7	1.0237	9	0.7
Mixed deciduous and Sassafras	978.8	0.5376	35	0.93
Eucalyptus	887.3	0.4554	20	0.8
Casuarina	744.1	3.2377	10	0.95
Populus	496.9	2.6973	13	0.92
Lucidophyllous forests	929.2	0.6494	24	0.83
Nonmerchantable woods	1178.3	0.2559	17	0.95
Mixed conifer and deciduous	813.6	1.8466	10	0.99
Tropical forests	797.5	0.042	18	0.87

BGD
12, 19535–19577, 2015
Modeling the uncertainty of estimating forest carbon stocks in China
T. X. Yue et al.

Table 3. CFs of each forest type in China (Li and Lei, 2010).

Forest type	CF	Forest type	CF	Forest type	CF
Pinuskoraiensis	0.5113	*Pinusyunnanensis*	0.5113	*Tilia*	0.4392
Abiesfabri	0.4999	*Pinuskesiya* var. *langbianensis*	0.5224	*Sassafras tzumu*	0.4848
Piceaasperata	0.5208	*Pinusdensata*	0.5009	*Eucalyptus robusta* Smith	0.5253
Tsugachinensis	0.5022	*Cunninghamialanceolata*	0.5201	*Casuarinaequisetifolia*	0.4980
Cupressusfunebris	0.5034	*Cryptomeriafortunei*	0.5235	*Populus*	0.4956
Larixgmelinii	0.5211	Metasequoiaglyptostroboides	0.5013	*Firmiana*	0.4695
Pinussylvestris var. *mongolica*	0.5223	Coniferous mixed forest	0.5101	Nonmerchantable woods	0.4834
Pinusdensiflora	0.5141	Broad-leaved and coniferous mixed forest	0.4978	Broad-leaved mixed forest	0.4900
Pinusthunbergii	0.5146	*Fraxinusmandschurica*, *Juglansmandshurica*, *Phellodendronamurense*	0.4827	Coppice	0.5000
Pinustabuliformis	0.5207	*Cinnamomumcamphora*	0.4916		
Pinusarmandii	0.5225	*Phoebe zhennan*	0.5030		
Keteleeriafortunei	0.4997	Oaks	0.5004		
Pinusmassoniana	0.4596	*Betula*	0.4914		

BGD
12, 19535–19577, 2015

Table 4. Comparison of carbon estimates and errors produced with the five different methods.

Methods	AMCS (Pg)	MAE ($kg\,m^{-2}$)	MRE (%)
LPJ	10.53	3.12	79.33
Kriging	7.26	1.97	50.12
SOA	6.55	1.92	48.77
HASM-LPJ	7.34	1.23	31.26
HASM-SOA	7.08	0.89	22.71

BGD
12, 19535–19577, 2015

Table 5. Mean annual carbon stocks and carbon densities in China estimated with the five different methods.

Method	Calculation object	Coniferous forests	Mixed forests	Broadleaf forests	Total
LPJ	AMCS (Pg)	3.82	0.57	6.14	10.53
	AMCD ($kg\,m^{-2}$)	6.06	6.18	7.38	
SOA	AMCS (Pg)	2.48	0.46	3.61	6.55
	AMCD ($kg\,m^{-2}$)	3.94	4.93	4.34	
Kriging	AMCS (Pg)	2.76	0.39	4.11	7.26
	AMCD ($kg\,m^{-2}$)	4.38	4.24	4.94	
HASM-LPJ	AMCS (Pg)	2.83	0.38	4.13	7.34
	AMCD ($kg\,m^{-2}$)	4.5	4.09	4.95	
HASM-SOA	AMCS (Pg)	2.74	0.39	3.95	7.08
	AMCD ($kg\,m^{-2}$)	4.35	4.2	4.74	

BGD
12, 19535–19577, 2015

BGD
12, 19535–19577, 2015

Table 6. MACS and MACD of the forests in the nine regions of China during the periods 2004–2008 and 1984–1988.

Regions	P5 (from 2004 to 2008)			P1 (from 1984 to 1988)		CS accumulation rate
	AMCD ($kg\,m^{-2}$)	AMCS (Pg)	Percentage (%)	AMCD ($kg\,m^{-2}$)	AMCS (Pg)	($Tg\,yr^{-1}$)
R1	3.710	0.28	3.94	2.666	0.16	6.2
R2	6.330	0.20	2.80	6.358	0.15	2.3
R3	4.445	2.01	28.41	4.493	1.59	21.3
R4	3.274	0.19	2.68	3.035	0.13	2.8
R5	10.525	2.03	28.61	6.718	0.99	52.0
R6	3.671	1.03	14.48	3.734	0.82	10.4
R7	3.693	0.42	5.89	3.643	0.36	2.9
R8	2.138	0.06	0.83	1.515	0.03	1.3
R9	2.598	0.87	12.26	2.358	0.62	12.7
Total		7.08	100		4.84	112

Table 7. MACSs and MACDs for all forest types during the five periods estimated using HASM-SOA.

Period	Calculation object	Deciduous coniferous forests	Evergreen coniferous forests	Broad-leaved and coniferous mixed forests	Deciduous broad-leaved forests	Evergreen broad-leaved forests
P1	AMCS (Pg)	0.41	1.50	0.06	1.38	0.63
	AMCD ($kg\,m^{-2}$)	4.35	3.81	3.08	3.75	4.35
P2	AMCS (Pg)	0.39	1.80	0.09	1.44	0.87
	AMCD ($kg\,m^{-2}$)	4.28	4.13	3.75	3.77	5.65
P3	AMCS (Pg)	0.44	2.23	0.07	1.66	1.20
	AMCD ($kg\,m^{-2}$)	4.20	4.09	3.03	3.87	6.35
P4	AMCS (Pg)	0.47	2.19	0.19	1.97	1.57
	AMCD ($kg\,m^{-2}$)	4.37	4.40	5.18	3.89	7.49
P5	AMCS (Pg)	0.40	2.34	0.39	2.11	1.84
	AMCD ($kg\,m^{-2}$)	3.77	4.47	4.20	3.93	6.22

BGD
12, 19535–19577, 2015

Table 8. MACSs and MACDs estimated for the whole China excluding Taiwan, Hong Kong and Macao during the five periods using HASM-SOA.

Periods	Area (million km^2)	AMCS (Pg C)	AMCD (kg C m^{-2})
P1	1.2101	4.84	4.001
P2	1.2864	5.55	4.315
P3	1.2920	5.60	4.334
P4	1.4279	6.38	4.469
P5	1.5559	7.08	4.55

BGD
12, 19535–19577, 2015

Modeling the uncertainty of estimating forest carbon stocks in China

T. X. Yue et al.

Table 9. MACSs and MACDs estimated for the five periods and nine regions with HASM-SOA.

Regions	P1		P2		P3		P4		P5	
	AMCD ($kg\,m^{-2}$)	AMCS (Pg)	AMCD ($kg\,m^{-2}$)	AMCS (Pg)	AMCD ($kg\,m^{-2}$)	AMCS (Pg)	AMCD ($kg\,m^{-2}$)	AMCS (Pg)	AMCD ($kg\,m^{-2}$)	AMCS (Pg)
R1	2.67	0.16	2.71	0.17	2.88	0.17	2.98	0.20	3.71	0.28
R2	6.36	0.15	6.27	0.16	6.25	0.15	6.23	0.18	6.33	0.20
R3	4.49	1.59	4.42	1.64	4.50	1.64	4.43	1.77	4.44	2.01
R4	3.04	0.13	3.23	0.15	3.13	0.14	3.15	0.16	3.27	0.19
R5	6.72	0.99	10.15	1.57	10.83	1.64	11.49	1.94	10.53	2.03
R6	3.73	0.82	3.78	0.87	3.66	0.82	3.88	0.96	3.67	1.03
R7	3.64	0.36	3.79	0.39	3.66	0.37	3.54	0.40	3.69	0.42
R8	1.52	0.03	1.64	0.04	1.89	0.04	1.89	0.05	2.14	0.06
R9	2.36	0.62	2.05	0.56	2.30	0.62	2.51	0.73	2.60	0.87
The whole of China	4.00	4.84	4.32	5.55	4.33	5.60	4.47	6.38	4.55	7.08

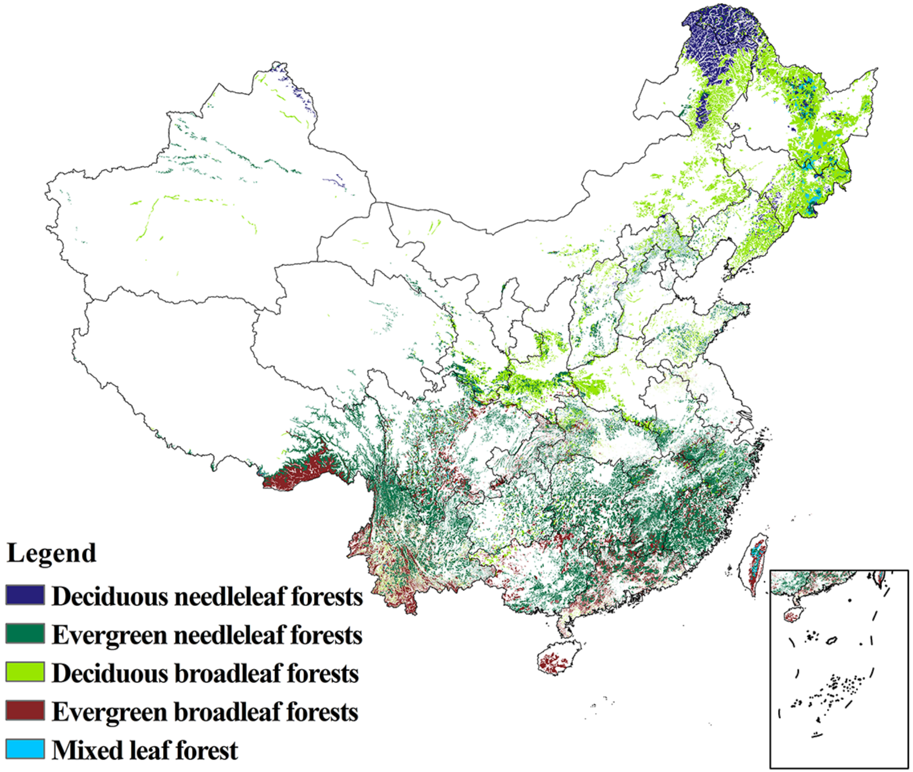

Figure 1. The updated forest cover map of in China.

BGD
12, 19535–19577, 2015

Modeling the uncertainty of estimating forest carbon stocks in China

T. X. Yue et al.

Title Page
Abstract | Introduction
Conclusions | References
Tables | Figures
◀| |▶
◀ ▶
Back | Close
Full Screen / Esc
Printer-friendly Version
Interactive Discussion

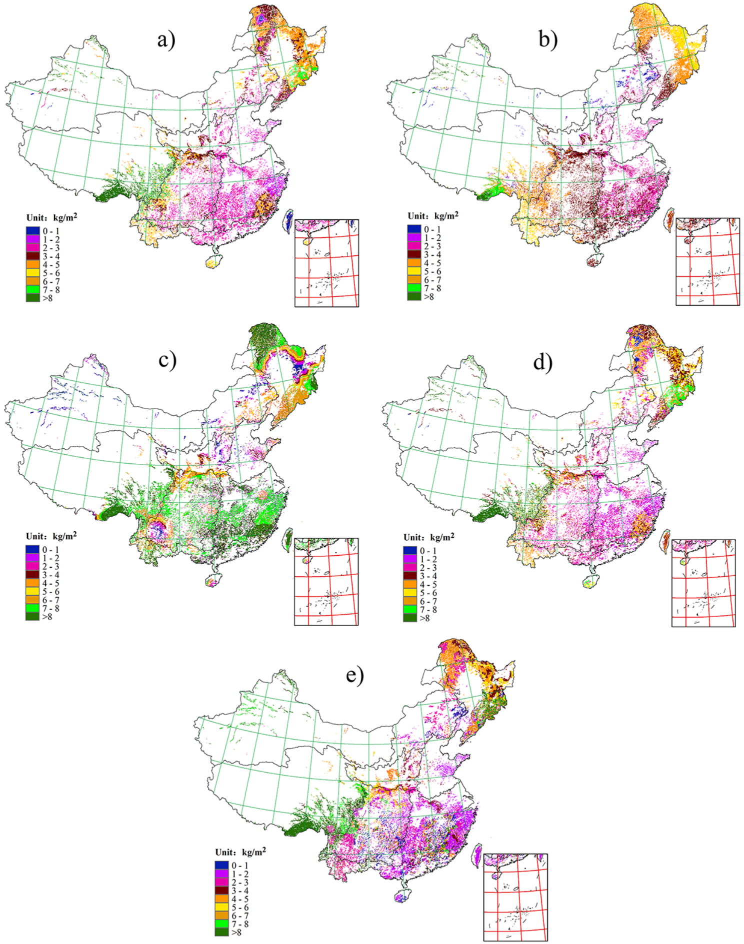

Figure 2. The spatial distribution of forest biomass MACDs estimated during the period 2004–2008 in China using: **(a)** Kriging; **(b)** SOA; **(c)** LPJ; **(d)** HASM-SOA; and **(e)** HASM-LPJ.

BGD
12, 19535–19577, 2015

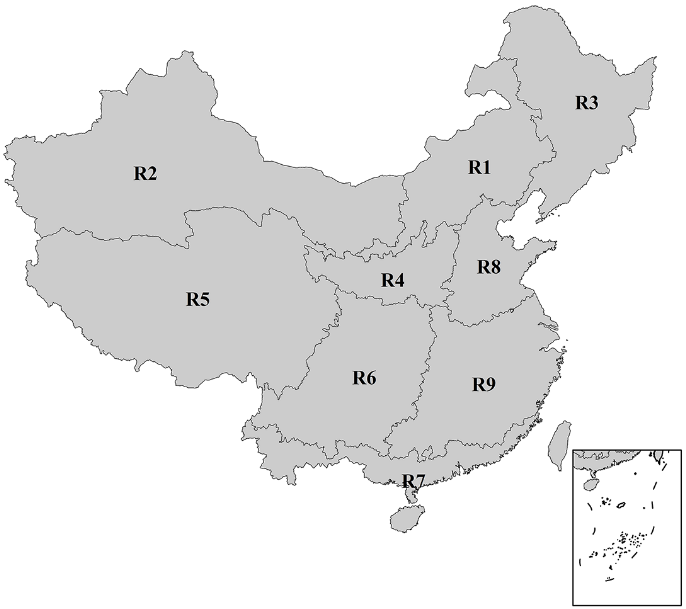

Figure 3. Map showing the nine regions of China used for detailed analysis.

BGD
12, 19535–19577, 2015

Modeling the uncertainty of estimating forest carbon stocks in China

T. X. Yue et al.

Title Page
Abstract | Introduction
Conclusions | References
Tables | Figures
◂ | ▸
Back | Close
Full Screen / Esc
Printer-friendly Version
Interactive Discussion

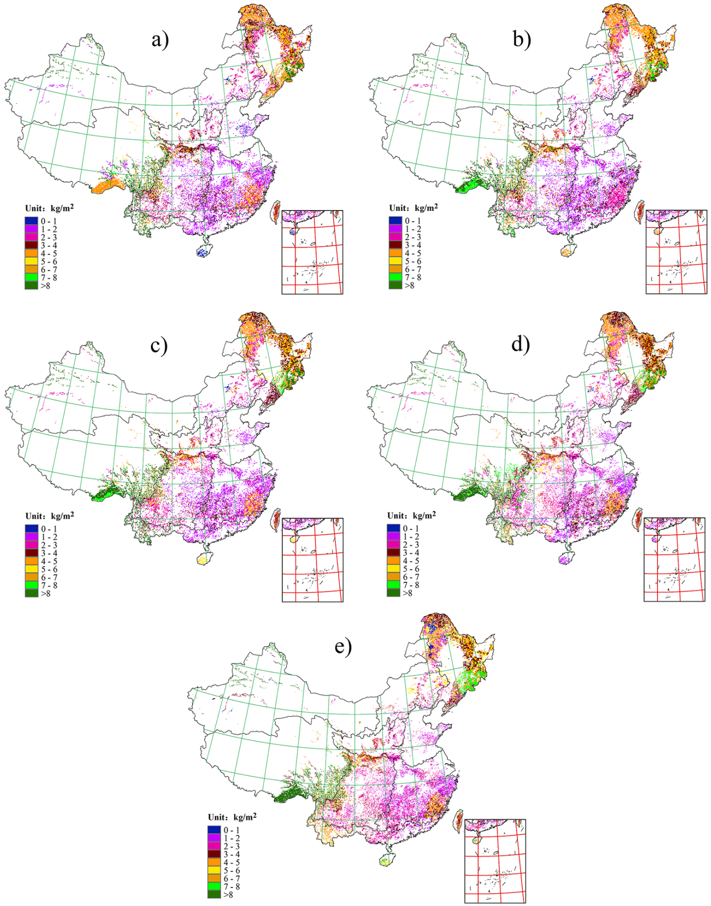

Figure 4. The spatial distribution of forest MACDs in China estimated during the five periods using HASM-SOA: **(a)** 1984–1988 (P1); **(b)** 1989–1993 (P2); **(c)** 1994–1998 (P3); **(d)** 1999–2003 (P4); and **(e)** 2004–2008 (P5).

BGD
12, 19535–19577, 2015